On the Mechanism of Conversion of *N*-Acyl-4-acyloxy-*β*-lactams into 2-Substituted 1,3-Oxazin-6-ones. Can a Low-Barrier Transition State Be Antiaromatic?

Mateo Alajarín* and Pilar Sánchez-Andrada

Departamento de Química Orgánica, Facultad de Química, Campus de Espinardo, Universidad de Murcia, 30100 Murcia, Spain

Fernando P. Cossío* and Ana Arrieta

Kimika Fakultatea, Euskal Herriko Unibertsitatea, P. K. 1072, 20080 San Sebastián-Donostia, Spain

Begoña Lecea

Farmazi Fakultatea, Euskal Herriko Unibertsitatea, P. K. 450, 01080 Vitoria-Gasteiz, Spain

qopcomof@sq.ehu.es

Received July 12, 2001

The mechanism of the conversion of *N*-acyl-4-acyloxy-*β*-lactams into 1,3-oxazin-6-ones has been investigated using ab initio and density functional theories. It has been found that two pseudopericyclic reactions are involved in the whole process. The first key reaction is a retro-[*4-exo-dig*] cyclization instead of a thermal conrotatory electrocyclic ring opening. Magnetic characterization of the corresponding transition structure shows antiaromatic character, despite the low activation energy associated with this process. The second step is very exothermic and has no activation barrier. It corresponds to another pseudopericyclic reaction instead of a six-electron disrotatory electrocyclization. These results confirm that there is no correlation between aromaticity and pseudopericyclic reactions. In contrast, thermal-symmetry-allowed pericyclic reactions are always aromatic. Therefore, magnetic analysis of the corresponding transition structures constitutes a useful tool to distinguish between both kinds of processes.

Introduction

We have recently described[1] the one-step conversion of 4-acyloxy-*β*-lactams **1** into 2-substituted 1,3-oxazin-6-ones **2**, which are versatile intermediates in heterocyclic synthesis (Scheme 1). We have proved the validity of this methodology employing a variety of acyl chlorides (aroyl, heteroaroyl, alkenoyl, and alkanoyl).

These reactions take place by initial formation of *N*-acyl-4-acyloxy-*β*-lactams, which are subsequently transformed into 1,3-oxazin-6-ones by the action of the base. We have proposed a reasonable mechanistic explanation for the overall process. First the organic base promotes the *β*-elimination of carboxylic acid across the C3−C4 bond of *N*-acyl-4-acyloxy-*β*-lactam **3** yielding *N*-acylazetone **4**, which in a second step rapidly undergoes a four-centered electrocyclic ring opening to give the *N*-acylimidoylketene **5**. This compound then undergoes a six-centered electrocyclic closure yielding finally the 1,3-oxazin-6-one **2** (Scheme 2).

Experiments carried out in our laboratory are consistent with an E1cB-like mechanism for the *β*-elimination.[1] The participation of reactive intermediates **4** and **5** could not be unequivocally proved. However, this mechanism is supported by several facts: the most general methods for the synthesis of 1,3-oxazin-6-ones have been proposed

Scheme 1

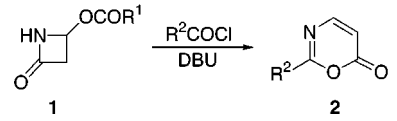

1 2

Scheme 2

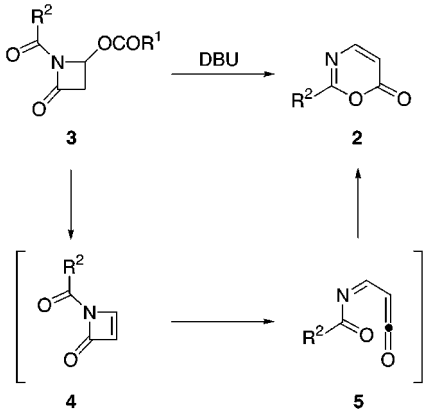

3 2

4 5

to involve, as immediate precursors, ring-opened valence tautomers such as *N*-acylimidoylketenes type **5**,[2] although they have never been isolated or detected by spectroscopic means. Two recent reports on this subject are coincident in that proposal.[3,4] With respect to the

* To whom correspondence should be addressed. E-mail for M.A.: alajarin@um.es.

(1) Alajarín, M.; Vidal, A.; Sánchez-Andrada, P.; Tovar, F.; Ochoa, G. *Org. Lett.* **2000**, *2*, 965.

(2) Steglich, G.; Jeschke, R.; Buschmann, E. *Gazz. Chim. Ital.* **1986**, *116*, 361.

10.1021/jo015922e CCC: $20.00
Published on Web 11/13/2001

intermediate *N*-acylazetone **4**, it is worth pointing out that azetones have occasionally been proposed in the literature as highly reactive intermediates.[5−7] The intraanular amide resonance leads to formally antiaromatic structures, and they have only been well-characterized in their benzo-fused forms,[8,9] whereas Wentrup et al. claimed the isolation of an *N*-adamantylazetone in Ar matrix at 77 K together with its ring-opened valence tautomer imidoylketene.[10]

Pericàs et al. published in 1986 an article questioning whether *N*-acylazetones can ever be obtained.[11] The authors reported the impossibility to prepare *N*-acylazetones by [2+2] cycloaddition of benzoyl isocyanate with di-*tert*-butoxyethyne. Instead they isolated the corresponding 1,3-oxazin-6-one as the main reaction product, and a mechanism similar to that described above was proposed for the conversion of *N*-acylazetones into 1,3-oxazin-6-ones. On the basis of semiempirical MNDO calculations they concluded that this conversion would take place easily and completely, even at low temperatures. The computed barrier for the conversion of *N*-formylazetone to *N*-formylimidoylketene was 16.2 kcal/mol, and 8.5 kcal/mol for the ring closure into 1,3-oxazin-6-one. On the other hand, the authors suggested that the highly stable *N*-acylazetones reported by Arbuzov and co-workers,[12−14] obtained from the reactions of benzoyl-isocyanate with several alkynes, are in fact 1,3-oxazin-6-ones.

Nguyen et al. have carried out ab initio calculations showing that the energy barrier for the ring opening of the parent azetone to the unsubstituted imidoylketene is 12.5 kcal/mol (MP2/6-31G**//HF/6-31G*), being an exothermic process (−10.0 kcal/mol).[15] More recently a study about the mechanism of ring opening of azetone using DFT methods has been published, the computed energy barrier at the B3LYP/6-31++G** level being 7.7 kcal/mol.[16]

We present herein the results of the theoretical calculations on the reaction path leading to 1,3-oxazin-6-one from *N*-formylazetone. Besides our own interest to understand how this process takes place, the discovery that two pseudopericyclic reactions are involved in the key steps of this sequence is interesting. The pseudopericyclic processes are a striking kind of pericyclic reactions that remained almost ignored for about 20 years but which have been placed on a solid foundation due to the recent works of Birney[17−22] and others.[23−26]

Computational Details

The ab initio orbital calculations were performed using Gaussian98 suite of programs.[27] Geometry optimizations were carried out at the RHF/6-31G* level and at the Becke3LYP[28−31] and MP2[32−36] theoretical levels with the internal 6-31+G* and 6-311++G** basis sets.[37] Harmonic frequency calculations at each level of theory verified the identity of each stationary point as a minimum or a transition state, and were used to provide an estimation of the zero-point vibrational energies (ZPVE), which were not scaled. Bond orders[38] and natural charges were calculated with the natural bond orbital (NBO) method.[39−41]

Results and Discussion

With the aim of simplifying the discussion we will discuss only the results obtained at the B3LYP/6-311++G** theoretical level, otherwise stated. The relative energies of all the stationary points reported in this

(3) McNab, H.; Withell, K. *Tetrahedron* **1996**, *2*, 3163.
(4) Millan, D. S.; Prager, R. H. *J. Chem. Soc., Perkin Trans. 1* **1998**, 3245.
(5) Kato, H.; Wakao, K.; Yamada, A.; Mutoh, Y. *J. Chem. Soc., Perkin Trans. 1* **1998**, 189.
(6) Kappe, T.; Zadeh, R. K. *Synthesis* **1975**, 247.
(7) Micetich, R. G.; Maiti, S. N.; Tanaka, M.; Yamazaki, T.; Ogawa, K. *J. Org. Chem.* **1986**, *51*, 853.
(8) Olofson, R. A.; Vander Meer, R. K.; Hoskin, D. H.; Bernheim, M.; Stournas, S.; Morrison, D. S. *J. Org. Chem.* **1984**, *49*, 3367.
(9) Wentrup, C.; Gross, G. *Angew. Chem., Int. Ed. Engl.* **1983**, *22*, 543.
(10) Kappe, C. O.; Kollenz, G.; Netsch, K.-P.; Leung-Toung, R.; Wentrup, C. *J. Chem. Soc., Chem. Commun.* **1992**, 488.
(11) Pericás, M. A.; Serratosa, F.; Valentí, E.; Font-Altaba, M.; Solans, X. *J. Chem. Soc., Perkin Trans. 2* **1986**, 961.
(12) Arbuzov, B. A.; Zoboya, N. N. *Dokl. Akad. Nauk. SSSR* **1967**, *172*, 845.
(13) Arbuzov, B. A.; Zoboya, N. N.; Balanova, F. B. *Izv. Akad. Nauk. SSSR., Ser. Khim.* **1970**, 1570.
(14) Arbuzov, B. A.; Zoboya, N. N.; Balanova, F. B. *Izv. Akad. Nauk. SSSR., Ser. Khim.* **1971**, 577.
(15) Nguyen, M. T.; Ha, T.; O'Ferral, R. A. M. *J. Org. Chem.* **1990**, *55*, 3251
(16) Fang, D.-C.; Ding, W.-J. *THEOCHEM* **1999**, *468*, 119.
(17) Birney, D. M. *J. Org. Chem.* **1996**, *61*, 243.
(18) Birney, D. M.; Xu, X.; Ham, S. *Angew. Chem., Int. Ed. Engl.* **1999**, *38*, 189.
(19) Birney, D. M.; Xu, X.; Ham, S.; Huang, X. *J. Org. Chem.* **1997**, *62*, 7114.
(20) Birney, D. M.; Ham, S.; Unruh, G. R. *J. Am. Chem. Soc.* **1997**, *119*, 4509.
(21) Ham, S.; Birney, D. M. *J. Org. Chem.* **1996**, *61*, 3962.
(22) Birney, D. M.; Wagenseller, P. E. *J. Am. Chem. Soc.* **1994**, *116*, 6262.
(23) Fabian, W. M. F.; Kappe, C. O.; Bakulev, V. A. *J. Org. Chem.* **2000**, *65*, 47.
(24) Fabian, W. M. F.; Bakulev, V. A.; Kappe, C. O. *J. Org. Chem.* **1998**, *63*, 5801.
(25) Liu, R. C.-Y.; Lusztyk, J.; McAllister, M. A.; Tidwell, T. T.; Wagner, B. D. *J. Am. Chem. Soc.* **1998**, *120*, 6247.
(26) Luo, L.; Bartberger, M. D.; Dolbier, W. R. *J. Am. Chem. Soc.* **1997**, *119*, 12366.
(27) Frisch, M. J.; Trucks, G. W.; Schlegel, H. B.; Scuseria, G. E.; Robb, M. A.; Cheeseman, J. R.; Zakrzewski, V. G.; Montgomery, J. A., Jr.; Stratmann, R. E.; Burant, J. C.; Dapprich, S.; Millam, J. M.; Daniels, A. D.; Kudin, K. N.; Strain, M. C.; Farkas, O.; Tomasi, J.; Barone, V.; Cossi, M.; Cammi, R.; Mennucci, B.; Pomelli, C.; Adamo, C.; Clifford, S.; Ochterski, J.; Petersson, G. A.; Ayala, P. Y.; Cui, Q.; Morokuma, K.; Malick, D. K.; Rabuck, A. D.; Raghavachari, K.; Foresman, J. B.; Cioslowski, J.; Ortiz, J. V.; Stefanov, B. B.; Liu, G.; Liashenko, A.; Piskorz, P.; Komaromi, I.; Gomperts, R.; Martin, R. L.; Fox, D. J.; Keith, T.; Al-Laham, M. A.; Peng, C. Y.; Nanayakkara, A.; Gonzalez, C.; Challacombe, M.; Gill, P. M. W.; Johnson, B.; Chen, W.; Wong, M. W.; Andres, J. L.; Gonzalez, C.; Head-Gordon, M.; Replogle, E. S.; Pople, J. A. *Gaussian 98*, revision A.5; Gaussian, Inc.: Pittsburgh, PA, 1998.
(28) Parr, R. G.; Yang, W. *Density-Functional Theory of Atoms and Molecules*; Oxford University Press: New York, 1989.
(29) Bartolotti, L. J.; Fluchichk, K. *Reviews in Computational Chemistry*; Lipkowitz, K. B.; Boyds D. B., Eds.; VCH Publishers: New York, 1996; Vol. 7, pp 187−216.
(30) Kohn, W.; Becke, A. D.; Parr, R. G. *J. Phys. Chem.* **1986**, *100*, 12974.
(31) Ziegler, T. *Chem. Rev.* **1991**, *91*, 651.
(32) Moller, C.; Pleset, M. S. *Phys. Rev.* **1934**, *46*, 618.
(33) Frisch, M. J.; Head-Gordon, M.; Pople, J. A. *Chem. Phys. Lett.* **1990**, *166*, 281.
(34) Frisch, M. J.; Head-Gordon, M.; Pople, J. A. *Chem. Phys. Lett.* **1990**, *166*, 275.
(35) Binkley, J. S.; Pople, J. A. *Int. J. Quantum Chem.* **1975**, *9*, 229.
(36) Pople, J. A.; Binkley, J. S.; Seeger, R. *Int. J. Quantum Chem. Symp.* **1976**, *10*, 1.
(37) Hehre, W. J.; Radom, L.; Schleyer, P. v. R.; Pople, J. A. *Ab Initio Molecular Orbital Theory*; Wiley: New York, 1986; pp 71−82, and references therein.
(38) Wiberg, K. B. *Tetrahedron* **1968**, *24*, 1083.
(39) Redd, A. E.; Weinstock, R. B.; Weinhold, F. *J. Chem. Phys.* **1985**, *83*, 735.
(40) Reed, A. E.; Curtiss, L. A.; Weinhold, F. *Chem. Rev.* **1988**, *88*, 899.
(41) Reed, A. E.; Schleyer, P. v. R. *J. Am. Chem. Soc.* **1990**, *112*, 1434.

Table 1. Relative Energies[a] with Zero Point Vibrational Correction, Low or Imaginary Frequencies, and Dipole Moments of *N*-Formylazetones, *N*-Formylimidoylketenes, and Related Compounds

structure	RHF/6-31G*	B3LYP/6-311++G**	MP2/6-311++G**	low freq[b]	dipole moment[c]
4-SZ	33.88	30.48	28.58	113.8	5.50
4-SE	29.00	26.61	25.40	108.9	2.80
TS2a	43.63	42.27	37.99	−190.8	3.45
TS2b	45.02	42.73	38.58	−146.2	4.43
5-NZSZ[d]	20.12			129.5	2.47
5-NESZ	18.66	16.12	16.96	67.1	3.27
5-NESE	21.15	16.81	17.30	95.9	5.55
TS3a	44.49	32.39	33.04	−257.8	5.23
TS3b	40.56	30.11	31.73	−287.7	3.07
TS4	36.88	27.26	31.82	−248.2	5.23
2	0.00	0.00	0.00	106.6	2.39

[a] In kcal/mol, with ZPVE correction, the ZPEs not were scaled. [b] In cm^{-1} at the MP2/6-311++G** level, except for **5-NZSZ** which was calculated at the RHF/6-31G* level. Negative numbers indicate the imaginary frequency. [c] In debye at the MP2/6-311++G** level and at the same density, except for **5-NZSZ** which was calculated at the RHF/6-31G* level. [d] This molecule was not a stationary point at the MP2/6-311++G** and B3LYP/6-311++G** levels, see text for details.

Scheme 3

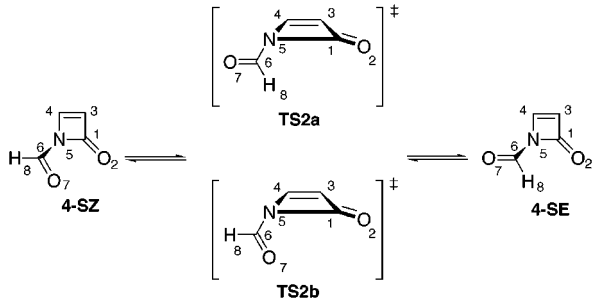

work and computed at different levels of theory are collected in Table 1. The most relevant geometrical parameters of these points are gathered in Table S1 of the Supporting Information.

***N*-Formylazetone.** We describe herein the two extreme rotamers of *N*-formylazetone around the exocyclic C−N amide linkage, **4-SE** and **4-SZ** (Scheme 3).

The frequency analysis confirmed both structures as minima, conformer SE being the most stable one by 3.18 kcal/mol. The computed dipole moment in the SZ rotamer (5.498 D) is notably greater than in **4-SE** (2.801 D). Therefore, the thermodynamic preference for the *E*-rotamer can be modified in polar solvents.

Regarding the structural features of azetones **4-SE** and **4-SZ**, the pyramidal geometry of the nitrogen atom in both rotamers at the MP2 theoretical level is remarkable, but notably disminished at B3LYP. The degree of pyramidalization can be measured by the sum $\sum\alpha$ of the bond angles at the nitrogen atom. Thus, $\sum\alpha$ is near to 360° for both rotamers at the B3LYP level ($\sum\alpha_{4-SE} = 358.79°$, $\sum\alpha_{4-SZ} = 358.03°$) showing an almost planar geometry. However, at the MP2 level these values decrease notably ($\sum\alpha_{4-SE} = 343.82°$, $\sum\alpha_{4-SZ} = 343.20°$).

The completely planar structures of **4-SE** and **4-SZ** were both characterized as transition structures for the nitrogen inversion at the MP2 level of theory. The calculated barriers to inversion were 0.57 and 0.50 kcal/mol for **4-SZ** and **4-SE**, respectively, at the MP2 level. At the B3LYP level, however, the difference in energy between the completely planar structure and the slightly pyramidalized minima is negligible (ca. 0.05 kcal/mol), thus indicating that **4-SE** and **4-SZ** can be considered as planar rotamers at room temperature.

If we compare the almost planar geometry of the unsubstituted azetidin-2-one[42] with that of unsubstituted azetone **6** pyramidalized at the nitrogen, the value of 5.8 kcal/mol reported by Nguyen[15] for the nitrogen inversion barrier of this last compound can be attributed to antiaromatic destabilization. Olofson and co-workers have reported the sole crystal structure of an azetone, the *N*-adamantylbenzazetone,[8] revealing a flat configuration with a sp^2 hybridization at the nitrogen center. In his paper, Nguyen pointed out that this feature, which apparently violates the classical Hückel's rule, may arise from a peculiar effect of the electron delocalization in the fused form.[15] Moreover, it is known that bulky substituents attached to the nitrogen lead to appreciable nonbonded repulsions. These interactions are stronger in the pyramidal than in the planar state, where repulsions are partially relieved by the opening of the internal angle. Thus, the presence of the adamantyl group in this compound also contributes to stabilize the flat geometry at the nitrogen.

We have studied the hypothetical antiaromatic character of azetone **6** and its N-formyl derivatives **4** using computational methods based on magnetic criteria.[43] In particular, we have calculated the nucleus-independent chemical shift[44] (NICS) of these species at different points. According to Schleyer,[44] large negative NICS values at the center of the ring under consideration are associated with aromatic character, whereas positive NICS values are a convenient indicator of antiaromaticity. In previous papers,[45−47] we have found that the behavior of aromatic compounds or transition states can be described by the variation of the NICS at different points above and below the molecular plane, the intersection point being the (3,+1) ring point of electron density as defined by Bader.[48] Thus, in-plane aromatic character is characterized by one ring current circulating along the

(42) Yang, Q.-C.; Seiler, P.; Dunitz, J. D. *Acta Crystallogr., Sect. C* **1987**, *43*, 565. The crystal structure of this compound reveals an almost planar nitrogen atom ($\sum\alpha = 354°$). We have performed the optimization of this molecule at the RHF/6-31G* and B3LYP/6-311++G** levels and in both cases the optimized structure was completely planar.

(43) (a) Minkin, V. I.; Glukhovtsev, M. K.; Simikin, B. Y. *Aromaticity and Antiaromaticity: Electronic and Structural Aspects*; Wiley: New York, 1994; pp 63−74. (b) Schleyer, P. v. R.; Jiao, H. *Pure Appl. Chem.* **1996**, *68*, 209.

(44) Schleyer, P. v. R.; Maerker, C.; Dransfeld, A.; Jiao, H.; Hommes, N. J. R. v. E. *J. Am. Chem. Soc.* **1996**, *118*, 6317.

(45) Morao, I.; Cossío. F. P. *J. Org. Chem.* **1999**, *64*, 1868.

(46) Cossío, F. P.; Morao, I.; Jiao, H.; Schleyer, P. v. R. *J. Am. Chem. Soc.* **1999**, *121*, 6737.

(47) R. de Lera, A.; Alvarez, R.; Lecea, B.; Torrado, A.; Cossío, F. P. *Angew. Chem., Int. Ed.* **2001**, *40*, 557.

(48) Bader, R. F. W. *Atoms in Molecules-A Quantum Theory*; Clarendon Press: Oxford, 1990; pp 13−52.

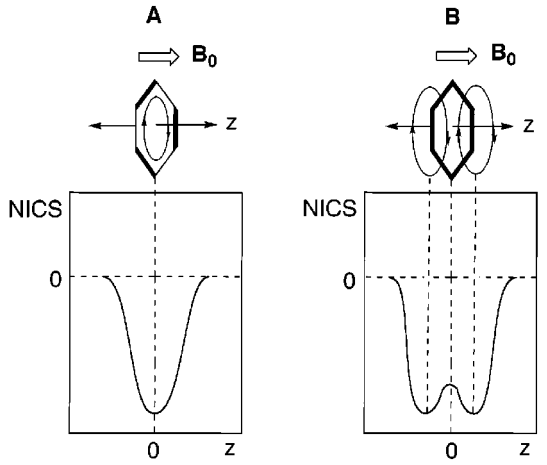

Figure 1. Different types of aromaticity. (A) Nucleus-independent chemical shift (NICS) vs *z* plot of the [2+2+2] cycloaddition of acetylene to form benzene, showing the maximum diamagnetic shielding at the molecular plane. (B) Nucleus-independent chemical shift (NICS) vs *z* plot of benzene, showing the maximum diamagnetic shielding above and below the molecular plane.

molecular plane of the cyclic structure under consideration. The transition structure of the [2+2+2] cycloaddition of three molecules of acetylene to form benzene is an example of this kind of aromaticity (Figure 1A). In contrast, two ring currents circulating at a certain distance from the molecular plane characterize π-aromaticity, benzene itself being the archetypical example (Figure 1B).

We have studied the behavior of the NICS of azetone in its pyramidalized form **6** and in the transition structure **TS1** associated with the nitrogen inversion. These results are outlined in Figure 2. According to our results (GIAO-B3LYP/6-31+G*//B3LYP/6-31+G* level), both forms of azetone exhibit positive NICS at all the points calculated. In the case of the pyramidalized form, the maximum is found in the neighborhood of the (3,+1) point, whereas the maximum paramagnetic NICS is found in **TS1** at ca. 0.9 Å above and below the molecular plane. This profile of the NICS along the axis perpendicular to the molecular plane of **TS1** is the antiaromatic equivalent of π^2-aromatic systems in which two diamagnetic ring currents circulate at ca. 0.5 Å above and below the molecular plane.[47] Although in this small ring it is difficult to discriminate the paratropic ring current from local paramagnetic effects,[43a] our results indicate that the planar azetone exhibits antiaromatic character (Figure 2).

In contrast, both conformers of *N*-formylazetone **4-SE** and **4-SZ** exhibit a lower antiaromaticity, as indicated by the magnitude and the shape of the NICS along the *z*-axis (Figure 3). Thus, the maximum NICS value for **4-SE** is found to be +3.75 ppm/mol at the (3,+1) ring point at the GIAO-B3LYP/6-31+G*//B3LYP/6-31+G* level. These results indicate that the amide resonance between the nitrogen atom and the exocyclic formyl group avoids partially the antiaromaticity arising from a cyclic array of four atoms and 4π electrons.

The equilibration between both rotamers **4-SE** and **4-SZ** can occur by rotation around the exocyclic amide linkage. Since rotation around the N−CHO bond temporarily destroys the exocyclic amide resonance, nonplanar transition structures result, denoted as **TS2a** and

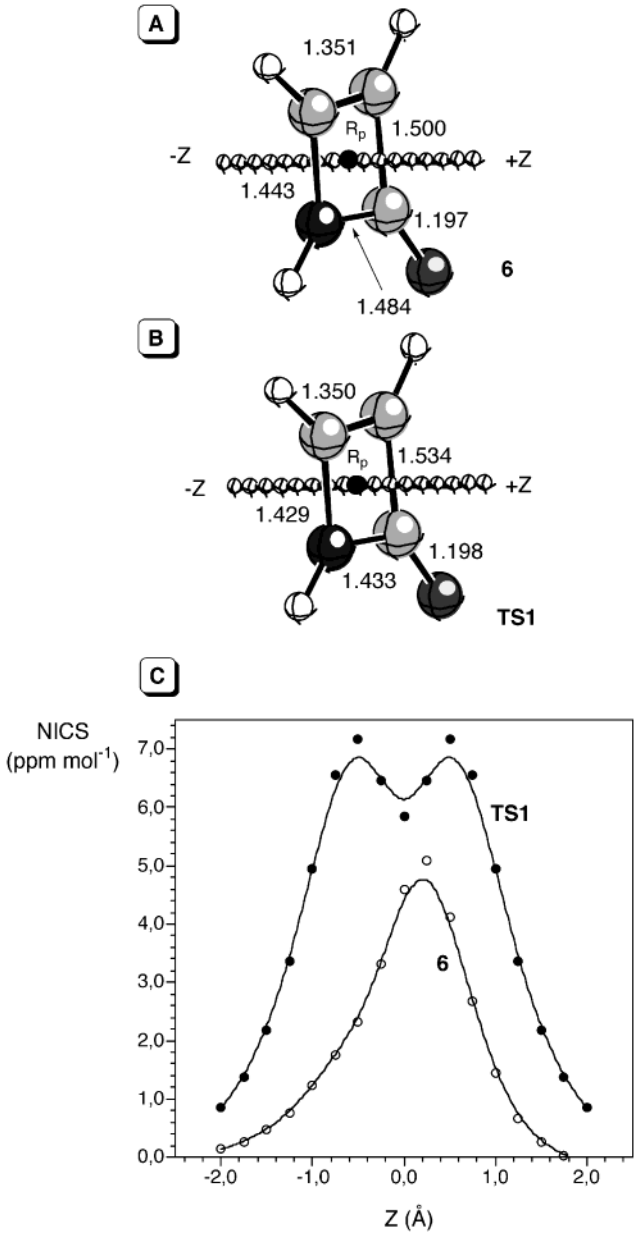

Figure 2. Main geometric features of azetone **6** (A) and its transition structure **TS1** (B) associated with the inversion of the nitrogen atom. Both sets of structural data correspond to the B3LYP/6-311+G** optimized geometries. Bond distances are given in angstroms (Å). R_p stands for the (3,+1) ring point of electron density. The small spheres correspond to the points used in the evaluation of the NICS values. (C) Plot of the calculated NICS versus *z* for **6** and **TS1**. The NICS values have been computed at the GIAO-B3LYP/6-31+G* level. The *z* axis has been defined as depicted in panels A and B.

TS2b, depending upon the orientation of the exocyclic carbonyl group with respect to the azetone ring. The chief geometric features of these transition structures are reported in Figure 4.

According to our results, **TS2b** is slightly lower in energy than **TS2a** (see Table 1). The repulsive interactions arising from the proximity of the lone pair at the nitrogen atom and one lone pair at the oxygen of the exocyclic carbonyl group in **TS2a** account for its greater energy value. Both structures show a high degree of pyramidalization at the nitrogen ($\sum\alpha \approx 314°$ and 320° at the MP2 and B3LYP levels, respectively). This pyramidalization can be explained in the same terms used in

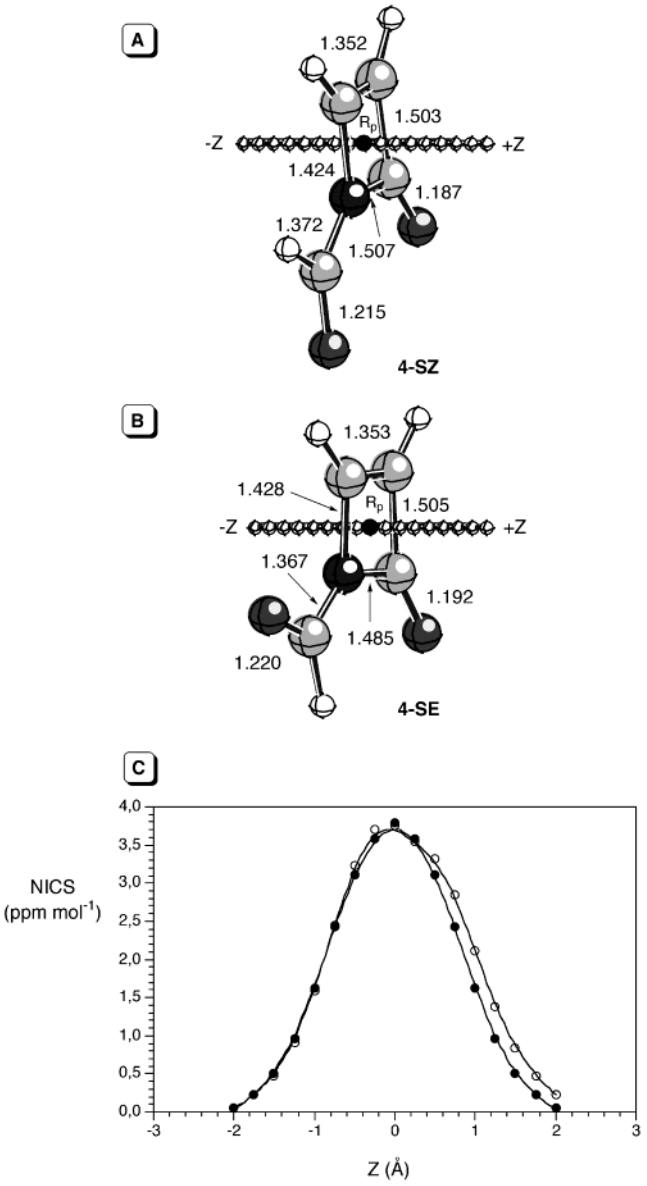

Figure 3. Main geometric features of rotamers **4-SZ** (A) and **4-SE** (B) of *N*-formylazetone. Both sets of structural data correspond to the B3LYP/6-311+G** optimized geometries. Bond distances are given in angstroms (Å). R_p stands for the (3,+1) ring point of electron density. The small spheres correspond to the points used in the evaluation of the NICS values. (C) Plot of the calculated NICS versus *z* for **6** and **TS1**. The NICS values have been computed at the GIAO−B3LYP/6-31+G* level. The *z* axis has been defined as depicted in panels A and B. Open circles and squares correspond to **4-SZ** and **4-SE**, respectively.

the case of azetone, namely the necessity of avoiding the antiaromatic destabilization derived from the endocyclic amide resonance. The calculated energy barrier for the transformation of **4-SZ** into **4-SE** through **TS2b** is 11.79 kcal/mol, and 15.66 kcal/mol for the reverse process. The corresponding values for the conversion through **TS2a** are 12.25 and 16.12 kcal/mol, respectively.

Ring Opening of *N*-Formylazetone 4 to Iminoketene 5. According to our calculations, both rotamers of *N*-formylazetone, **4-SE** and **4-SZ**, can easily undergo ring opening to give *N*-formylimidoylketene **5**. We consider in this paper only three of the possible conformers of *N*-formylimidoylketene, all having a *s*-cis configuration

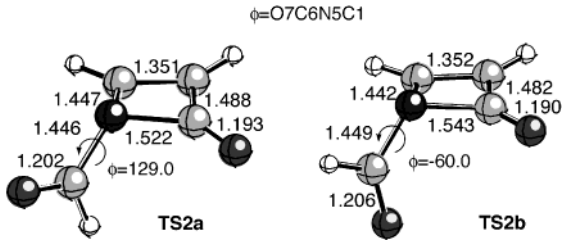

Figure 4. Transition structures **TS2a**,**b** associated with interconversion between rotamers **4-SZ** and **4-SE**. Bond distances and dihedral angles, calculated at the B3LYP/6-311+G** level, are given in angstroms (Å) and degrees, respectively.

Scheme 4

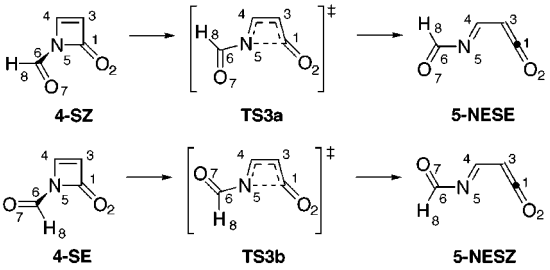

Scheme 5

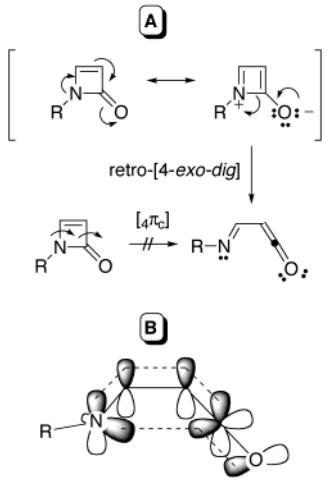

around the C3−C4 single bond. We name as NZ or NE the cis or trans geometry, respectively, of the C=N double bond and as SZ or SE the *s*-cis or *s*-trans conformation, respectively, around the N5−C6 single bond (Scheme 4).

The **4-SZ** rotamer experiences ring opening via **TS3a** yielding the **5-NESE** conformer, while **4-SE** undergoes the same process to give **5-NESZ** through **TS3b** (Scheme 4). This transformation can be envisaged as a four-electron conrotatory thermal electrocyclic ring opening[49] or as a reverse nucleophilic attack of the iminic nitrogen on the *sp*-hybridized ketene atom (Scheme 5A). This latter mechanism should correspond to a retro-[4-exo-dig] ring opening, in principle an unfavorable process according to the Baldwin rules.[50]

Our results unambiguously show that the geometric and electronic features of both transition structures do not correspond to those expected for a conrotatory mech-

(49) (a) Woodward, R. B.; Hoffmann, R. *The Conservation of Orbital Symmetry*; Academic Press: New York, 1970. (b) Dolbier, W. R., Jr.; Korionak, H.; Houk, K. N.; Sheu, C. *Acc. Chem. Res.* **1996**, *29*, 471.
(50) Baldwin, J. E. *J. Chem. Soc., Chem. Commun.* **1976**, 735.

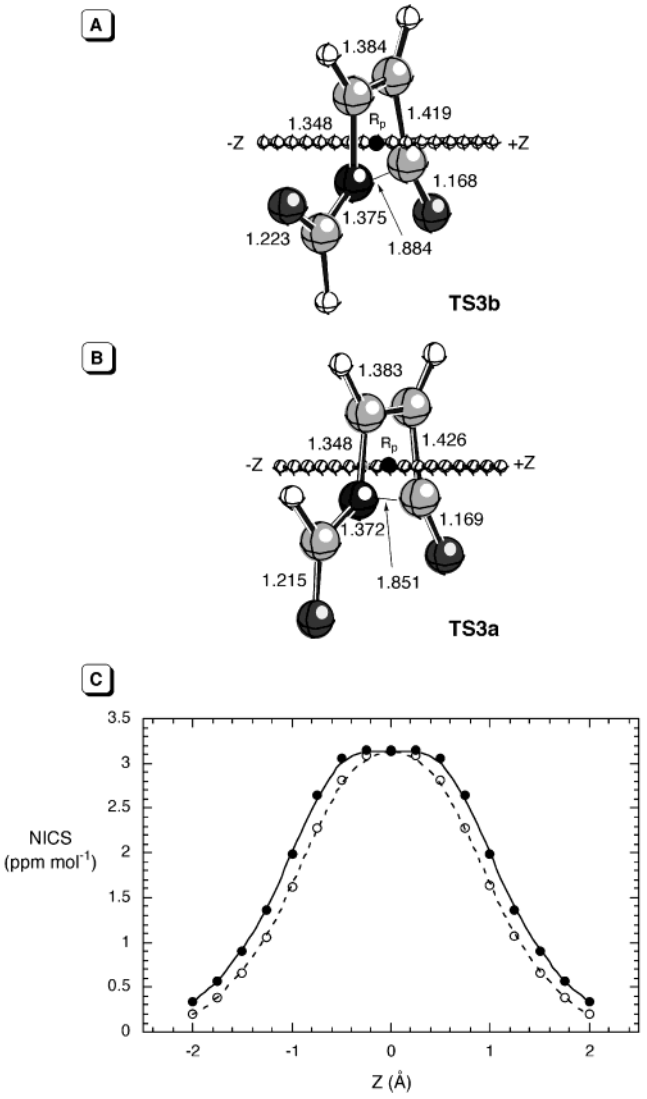

Figure 5. Main geometric features of transition structures **TS3b** (A) and **TS3a** (B) associated with the ring opening of both rotamers of *N*-formylazetone. Both sets of structural data correspond to the B3LYP/6-311+G** optimized geometries. Bond distances are given in angstroms (Å). R_p stands for the (3,+1) ring point of electron density. The small spheres correspond to the points used in the evaluation of the NICS values. (C) Plot of the calculated NICS versus *z* for **TS3a** (open circles) and **TS3b** (filled circles). The NICS values have been computed at the GIAO−B3LYP/6-31+G* level. The *z* axis has been defined as depicted in panels A and B.

anism. In particular, the harmonic analysis of both saddle points showed no torsion around the N5═C4 bond. Instead, the C_s symmetry of the transition structures is preserved along the imaginary vibration, thus resulting in a nonrotatory process (Figure 5). Therefore, our calculations show that **TS3a**,**b** are associated with a concerted process whose primary changes in bonding compass a cyclic array of atoms, where nonbonding and bonding atomic orbitals interchange their roles. There are "disconnections" in the cyclic array of overlapping orbitals because the atomic orbitals which have switching functions are mutually orthogonal (Scheme 5B). This corresponds to the Lemal's[51] definition of a pseudopericyclic process. This type of transformation cannot be orbital forbidden, regardless of the number of participant electrons.

We performed NICS calculations for **TS3a**,**b** along the axis that contains the ring point and is perpendicular to the molecular plane. The results are displayed in Figure 5. In effect, we have found positive values for the NICS along the *z*-axis, the values at the ring point being ca. +3.2 ppm mol^{-1} (GIAO-B3LYP/6-31+G* results). Thus, both transition structures show antiaromatic character. However, the computed energy barriers are very low: 3.51 kcal/mol for the ring opening of **4-SE** into **2-NESZ** and 1.91 for the conversion of **4-SZ** into **5-NESE**, both being exothermic processes. For the inverse process, i.e. the ring closure of **5-NESZ** into **4-SE**, the calculated energy barrier was 14.00 kcal/mol, and 15.57 kcal/mol for the ring closure of **5-NESE** into **4-SZ**. Therefore, in agreement with a previous paper,[47] we demonstrate that pseudopericyclic reactions do not correlate with aromaticity, whereas thermally allowed pericyclic reactions are always associated with aromatic transition structures.[52,53] Thus, magnetic characterization of transition states can distinguish between both kind of processes.

In summary, from these results it can be concluded that *N*-formylazetone experiences facile ring opening through a pseudopericyclic mechanism to give *N*-formylimidoylketene. The small height of the energy barriers calculated for the above process is due to the exothermicity of the reaction, the electrophilicity/nucleophilicity matching between the nitrogen atom and the carbonyl group, and the geometry constraints of the reactant that allow for appropriate angles in the transistion states. This result is in agreement with those reported by Birney[17,20,22] in other pseudopericyclic reactions.

Ring Closure of *N*-Formyliminoketenes 5 to 1,3-Oxazin-6-one 2. To investigate the mechanism of this last step, we studied first the isomerization of rotamers **5-NESE** and **5-NESZ** to the (*Z*)-imine analogue **5-NZSZ** (Figure 6A). We located the common transition structure **TS4**, in which the dihedral angles ω_1 = C1−C3−C4−N5 and ω_2 = O7−C6−N5−C1 are very close to 0° and −90°, respectively (Figure 6B). In general, two possible mechanisms can be envisaged for the isomerization of imines, namely rotation around the C═N bond and inversion at the nitrogen iminic atom.[54] We have only found the transition structure associated with the latter mechanism. This result is in agreement with a previous work on the isomerization of imines possessing π-electron-withdrawing groups such as *N*-methyleneformamide.[55] At the B3LYP level, the difference in energy between **TS4** and **5-NESZ** is only of 11.15 kcal/mol. Similarly, the energy barrier between **TS4** and **5-NESE** is of 10.45 kcal/mol. The relatively low energy of this transition structure can be explained taking into account the two-electron interaction between N5 and the π-acceptor formyl group. Thus, the NBO analysis shows a strong donation from

(51) Ross, J. A.; Seiders, R. P.; Lemal, D. M. *J. Am. Chem. Soc.* **1976**, *98*, 4325.

(52) (a) Herges, R.; Jiao, H.; Schleyer, P. v. R. *Angew. Chem., Int. Ed. Engl.* **1994**, *33*, 1736. (b) Jiao, H.; Schleyer, P. v. R. *Angew. Chem., Int. Ed. Engl.* **1995**, *34*, 334. (c) Jiao, H.; Schleyer, P. v. R. *J. Phys. Org. Chem.* **1998**, *11*, 655.

(53) (a) Evans, M. G. *Trans. Faraday Soc.* **1939**, *35*, 824. (b) Dewar, M. J. S. *The Molecular Orbital Theory of Organic Chemistry*; McGraw-Hill: New York, 1969; pp 316−339. (c) Zimmerman, H. *Acc. Chem. Res.* **1971**, *4*, 272.

(54) Eliel, E.; Wilen, S. H. *Stereochemistry of the Organic Compounds*; Wiley: New York, 1994; pp 550−555 and references therein.

(55) Allmann, R.; Kupfer, R.; Nagel, M.; Würthwein, E.-U. *Chem. Ber.* **1984**, *117*, 1597.

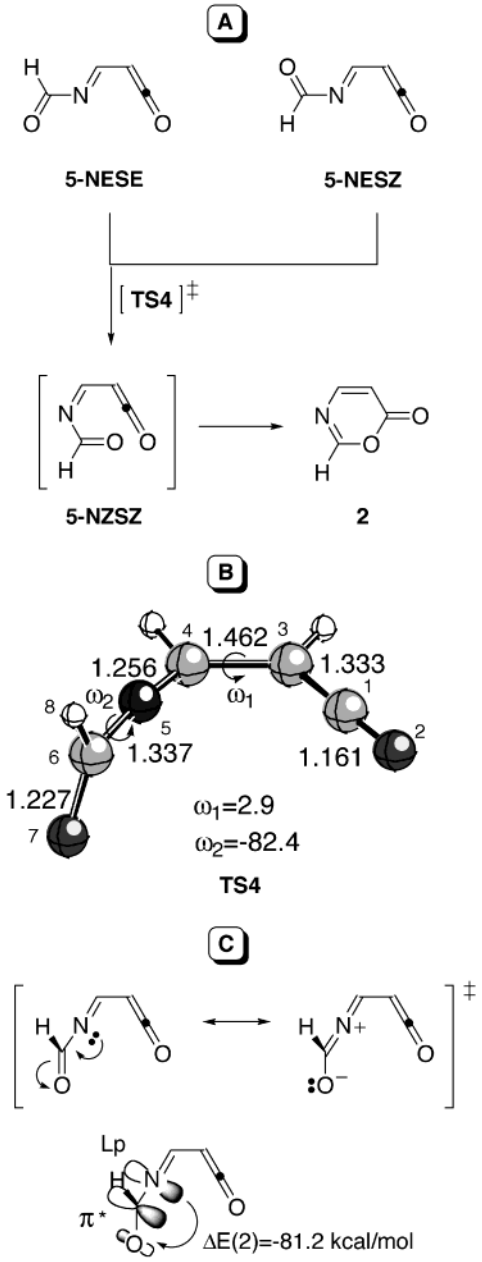

Figure 6. (A) Formation of 1,3-oxazin-6-one **2** from rotamers **5-NESE** and **5-NESZ**. (B) Main geometric features of **TS4**, computed at the B3LYP/6-311+G** level. Bond distances and angles are given in angstroms (Å) and degrees, respectively. (C) Resonance forms of **TS4** and second-order perturbation energy associated with donation from the lone pair of nitrogen to the π^* C=O natural localized orbitals.

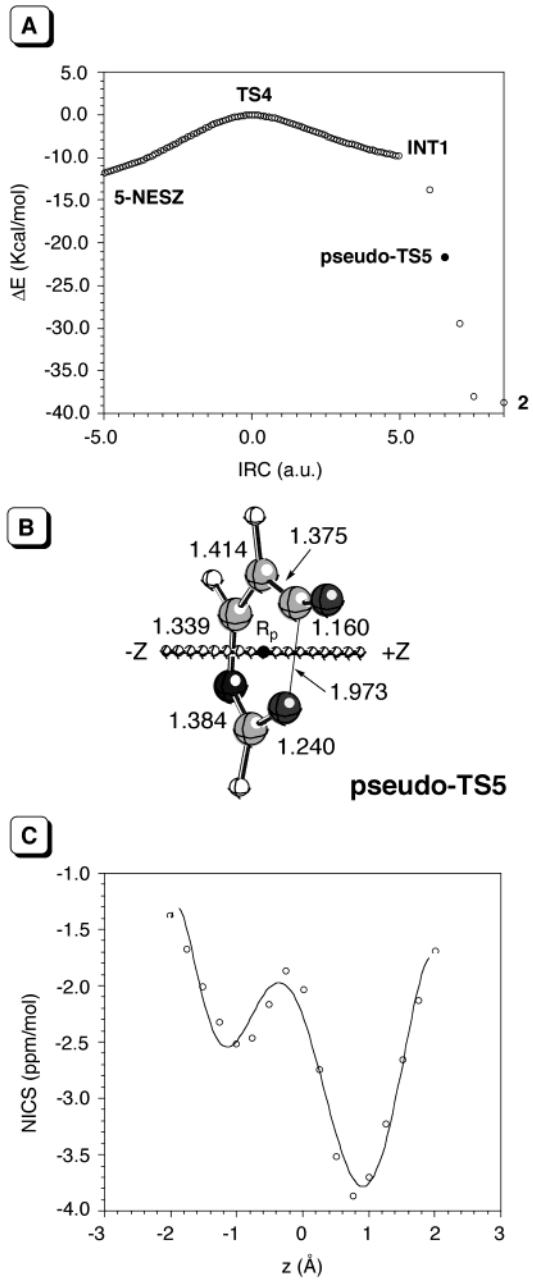

Figure 7. (A) Intrinsic reaction coordinate for the conversion of *N*-formylimino ketene **5-NESZ** to 1,3-oxazin-6-one **2**. Points beyond structure **INT1** do not correspond to the IRC but to the spontaneous convergence of this point to **2** during the optimization. **Pseudo-TS5** is the last intermediate point previous formation of the O−C bond. (B) Main geometric features of structures **pseudo-TS5**. These structural data correspond to the B3LYP/6-311+G** optimized geometry. Bond distances are given in angstroms (Å). R_p stands for the (3,+1) ring point of electron density. The small spheres correspond to the points used in the evaluation of the NICS values. (C) Plot of the calculated NICS versus *z* for **pseudo-TS5**. The NICS values have been computed at the GIAO-B3LYP/6-31+G* level. The *z* axis has been defined as depicted in panel B.

the lone pair of N5 to the π^* C6−O7 natural orbital (Figure 6C).

Extensive exploration of the potential energy surface around **TS4** did not allow to locate and characterize the isomer **5-NZSZ**. We have included in Figure 7A an intrinsic reaction coordinate (IRC) analysis performed starting from **TS4** to either **4-NESZ** or **2**. As it can be seen, all the attempts of optimization from the last point of the IRC converged to the reaction product 1,3-oxazin-6-one **2** without any activation barrier.[56] The absence of activation barrier for this process can be attributed to the fact that the weight of the energy barrier of a pseudopericyclic process depends greatly on the exothermicity of the reaction. As it can be seen in Table 1 and in Figure 7A, this is a highly exothermic reaction. In addition, there is a good matching between the reacting centers, the nucleophilic oxygen atom, and the electrophilic ketene central carbon atom. Therefore, **TS4** connects directly **5-NESE** and **5-NESZ** with the reaction product. To gain insight on the nature of the ring closure,

we have selected the last intermediate point before formation of the O−CO bond, denoted as **pseudo-TS5** in Figure 7, panels A and B. This almost planar structure has a nonaromatic character, as shown in Figure 7C. Instead of the in-plane aromatic profile expected for a disrotatory electrocyclization, we have obtained two small local minima along the *z*-axis perpendicular to the average molecular plane. Thus, in this latter case the minimum NICS is ca. −4 ppm/mol, whereas for a disrotatory electrocyclization involving 6 electrons the minimum NICS is ca. −13.6 ppm/mol.[47] This result indicates the presence of local diamagnetic effects in this second pseudopericyclic reaction, a result in line with those obtained for the cyclization of (*2Z*)-hexa-2,4,5-trienals and related compounds, with an average minimum NICS of ca. −7 ppm/mol.[47] Therefore, this second ring closure also confirms the absence of correlation between aromaticity and pseudopericyclic processes.

Conclusions

From the computational studies reported in this paper, we conclude that the conversion of *N*-acylazetones into 1,3-oxazin-6-ones takes place via two consecutive pseudopericyclic reactions. The first one consists of a retro-[*4-exo-dig*], whose associated transition structure has antiaromatic character. This can be attributed to the preservation of the partial antiaromaticity of the cyclic reactant. Despite this, the activation energy of this process is quite low, a remarkable result since [*4-exo-dig*] cyclizations are not favored according to the Baldwin rules. The second reaction can be described as a [*6-exo-dig*] cyclization instead of a disrotatory electrocyclization and is also a pseudopericyclic process, although the corresponding transition structure could not be located at correlated levels of theory. These results confirm that pseudopericyclic reactions can be associated with antiaromatic or nonaromatic transition structures. Since thermally allowed pericyclic reactions always correspond to aromatic transition states, magnetic characterization of these structures is a useful tool to distinguish between both general types of reactions.

Acknowledgment. The work in Murcia was supported by the DGES (Project PB95-1019), Fundación Séneca-CARM (Project PB/2/FS/99), and Acedesa (a division of Takasago). The work in San Sebastián-Donostia and Vitoria-Gasteiz was supported by the Gobierno Vasco/Eusko Jaurlaritza (Projects EX-1998-126 and PI-1998-116) and by Diputación Foral de Gipuzkoa/Gipuzkoako Foru Aldundia. P.S.-A. thanks Caja Murcia for a studentship and Ibon Alkorta (CSIC Madrid) for helpful discussions.

Supporting Information Available: Tables S1 and S2 including the chief geometric and energetic features of all stationary points discussed in the text. Cartesian coordinates of local minima and transition structures discussed in the text. This material is available free of charge via the Internet at http://pubs.acs.org.

JO015922E

(56) However, both **5-NZSZ** and the corresponding transition structure were located at the RHF/6-31G* level, although the activation barrier was calculated to be of only 0.06 kcal/mol.

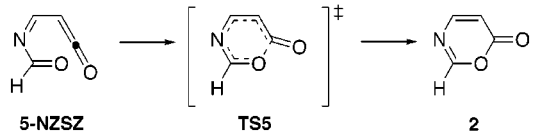

Harmonic and magnetic characterization of **TS5** (imaginary frequency = 223.4i cm^{-1}) confirmed that this saddle point does not correspond to a six-electron disrotatory thermal reaction, but to a pseudopericyclic π-aromatic [*6-exo-dig*] cyclization. Birney et al. have found an analogous reaction profile for the cyclization of vinylketene to 2-pyrone (see ref 17):